Prevost and Popescu (1996) state that for a constitutive model to be satisfactory it must be able to: 1) define the material behavior for all stress and strain paths; 2) identify model parameters by means of standard material tests; and 3) physically represent the material response to changes in applied stress or strain.

Previous studies have explored constitutive models and found that the use of isotropic models such as elasto-plastic Mohr-Coulomb and Drucker-Prager models are sufficiently accurate and easy to use.

The initial pre-construction at-rest earth pressures (Ko) was determined based on an assessment of the site history. The Mohr-Coulomb soil model was adopted for the soil layers, assuming fully drained conditions apply at all excavation stages. Effective soil friction angles (φ') and effective cohesion (c') were determined from consolidated drained triaxial tests. $E_{S0.1\text{-}0.2}$ presents compression modulus when the test pressure varied from 100 kPa to 200 kPa. In real soils, the stiffness depends significantly on the stress level, which means that the stiffness generally increases with depth. When using the Mohr-Coulomb model, the stiffness is a constant value. It should be noticed that using a constant stiffness modulus to represent soil behavior one should choose a value that is consistent with the stress level and the stress path development.

Table1. Typical input soil parameters

No.	Soil Name	Thickness（m）	Weight (kN/m^3)	void ratio *e*	Compression modulus $E_{S0.1\text{-}0.2}$(kN/m^2)	Efftive cohesion *c´*(kPa)	Effective friction angle *φ´*（°）	Hydraulic conductivity k_x（m/d）	k_y（m/d）
①1	Miscellaneous fill	1	18.0	--	--	--	--	--	--
②2	clayey silt	1	18.6	0.837	8160	6	24	0.0272	0.0502
③1	clayey silt	5.8	18.6	0.841	8900	5	26	0.0687	0.1132
④	mucky silt	5.8	16.7	1.430	2488	10	12	0.0001	0.0001
⑤1	Clay	3.8	17.3	1.200	2800	13	12	0.0001	0.0002
⑤2	clayey silt and Sandy clay	26.4	18.5	0.839	9900	5	32	0.1771	0.2894
⑦	Silty clay	8	18.5	0.857	9920	5	32.5	0.1426	0.2376
⑧1-1	silty clay	9.2	18	0.993	4550	16	19	0.0003	0.0006
⑧1-2	Silty sand	6	18.4	0.913	4810	18	20	0.02	0.02
⑧	Silty sand	4	18.5	0.84	7450	9	29	0.02	0.02

2				6					
⑨	silty clay	27	19.0	0.731	13130	3	35	0.02	0.02
⑩	Granite		--	--	--	--	--	--	--

The hydraulic conductivity (k) for the soils is varied in different directions. Table 1 shows the hydraulic conductivity in X (k_x) and Y(k_y). In all cases, the diaphragm wall-soil interface friction angle was assumed to be 0.5φ'. Table 1 summarizes the soil model parameters adopted in this finite element program.

The structure and soil strata are modeled in the 2D finite element program (input window as show in Fig.2). The model includes soil strata and structural element, like the diaphragm, the column and the beam. For considering the boundary conditions, the model is taken as 240m and 140m, two times width and one time depth than the basement.

An implicit integration of linear elastic perfectly plastic model which called Mohr-Coulomb model was used in the process of calculation. In this model the stress increments can generally be written as:

$$\Delta\sigma = D^e(\Delta\varepsilon - \Delta\varepsilon^p), \quad (1)$$

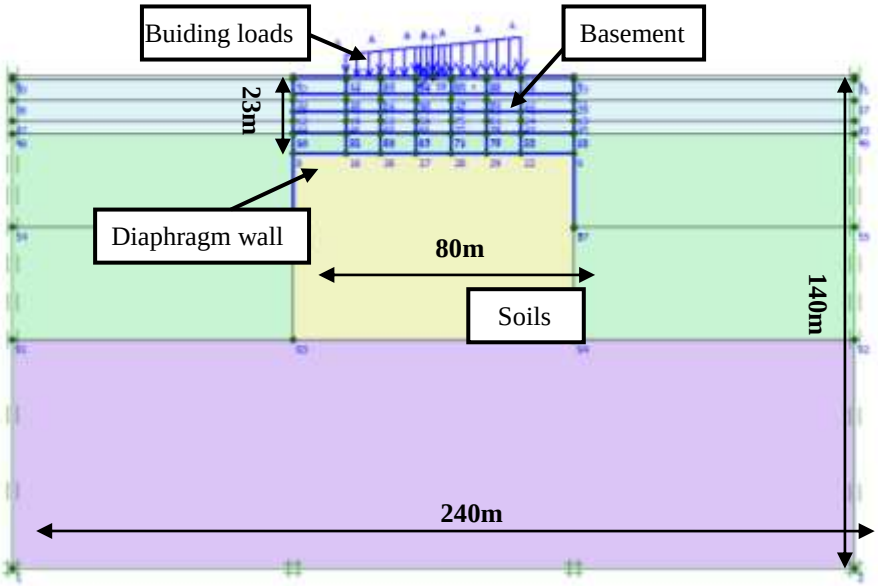

Fig.2 Numerical modeling

In this relation $\Delta\sigma$ represents the stress increment, D^e represents the elastic material matrix for the current increment. The strain increments are $\Delta\varepsilon$ obtained from the displacement increments using the strain interpolation matrix. For elastic material behavior, the plastic behavior, the plastic strain increment is zero. For plastic material behavior, the plastic strain increment $\Delta\varepsilon^p$ can be written as:

$$\Delta\varepsilon^{p} = \Delta\lambda\left[(1-\omega)(\frac{\partial g}{\partial\sigma})^{i-1} + \omega(\frac{\partial g}{\partial\sigma})^{i}\right], \quad (2)$$

In this equation $\Delta\lambda$ is the increment of the plastic multiplier and ω is a parameter indicating the type of time integration. For $\omega=1$ the integration is called implicit.

Biot's theory was used in this finite element program when considering the consolidation of the soils. Darcy's law for fluid flow and elastic behavior of the soil skeleton are also assumed.

4.2 structure models

The diaphragm walls and structural floors were modeled as elastic plate elements in finite element program, with full fixity at the connections. The contribution of the steel reinforcement in the concrete section was ignored. Table 2 summarizes the typical properties assumed for modeling the structural elements in program. γ represents the unit weight of the material. E presents elastic modulus, A presents the cross-section area, I represents geometrical moment of inertia.

Table2. Input parameters of structural element

Materials	models	$\gamma(kN/m^3)$	EA(kN/m)	EI (kN·m^2/m)
Diaphragm	Elasitc	25	4.20×10^7	5.04×10^6
column	Elasitc	25	5.04×10^7	6.05×10^6
Beams	Elasitc	25	1.75×10^7	3.68×10^5
Piles	Elasitc	25	6.62×10^6	5.98×10^5

5. Results

In this paper the base shear reaction and resisting capacity of diaphragm walls have been investigated using a new method for simulating this project. The results of the numerical analysis confirmed the diaphragm walls take the most of the base shear.

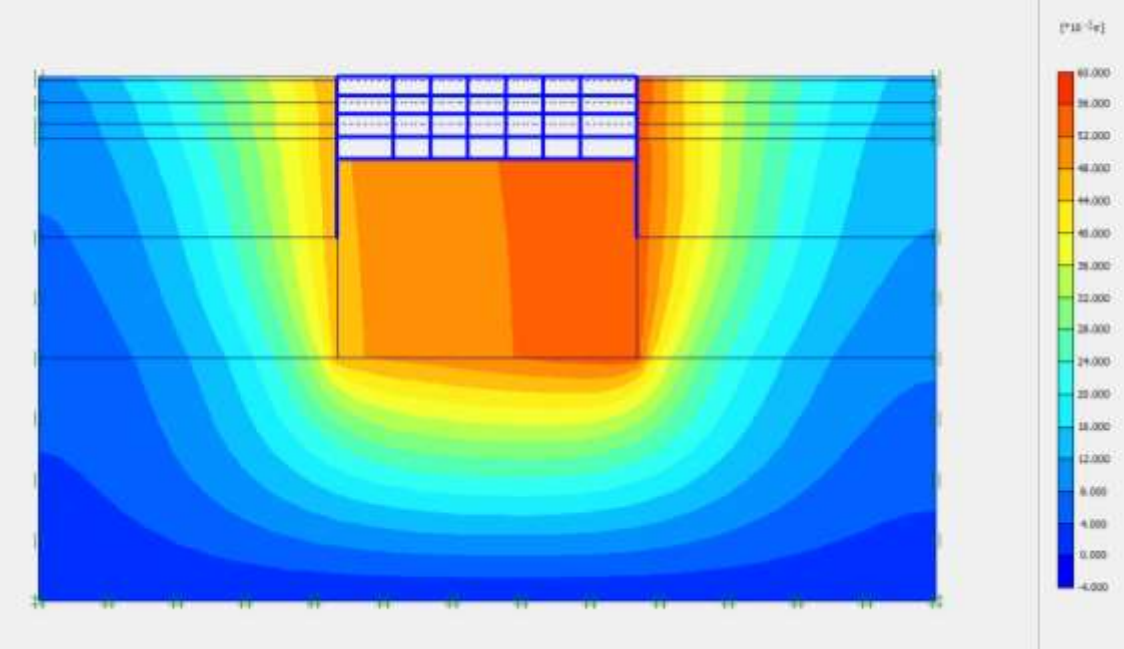

Fig.3 Displacement contour

The displacement contour of the deep foundation is shown in Fig.3. The results show that the deep foundation tilts to the right side under such loadings. The biggest settlement is about 56mm occurs in the top right of the basement. The soils in the right side of the basement are in a passive earth pressure area, while the left are in an active earth pressure area. And the deep foundation is in a balance state.

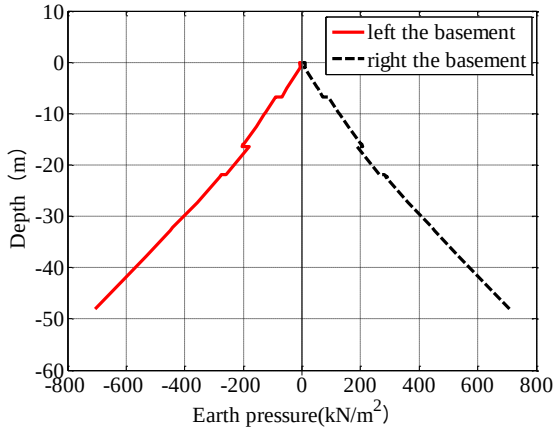

Fig.4 The earth pressure

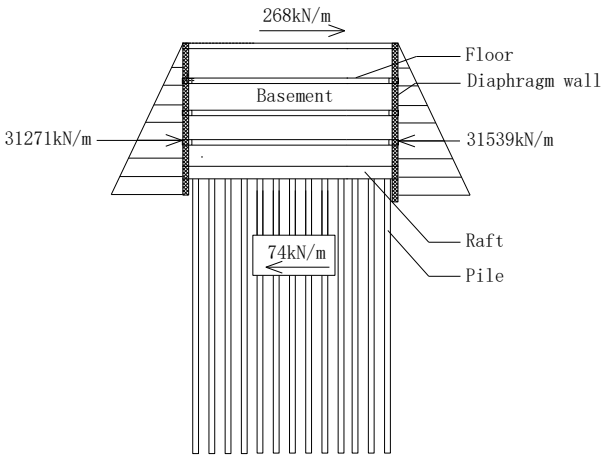

Fig.5 Horizontal loadings distribution

Fig.4 showed the earth pressures along the diaphragm walls. The pressure in active and passive pressure area has a similar distribution but different values. The total pressure in passive earth pressure area is bigger. And we calculate the total pressure in the left of the basement is 31271 kN/m, while 31539 kN/m in the right. While the horizontal loading transform from the upper structure is 268 kN/m. So we can easily judge that the piles bear the 74 kN/m. Each pile under the basement should be

assigned only about 28.9 kN. The piles even without special reinforcement can satisfy the practical requirement. The horizontal loadings are shown in Fig.5.

Table3. The reaction and resisting capacity of diaphragm wall and single pile

	Reaction(kN)	Resisting capacity(kN)	Proportion
Diaphragm wall	19400	140600	7.2%
Single pile	28.9	80.1	36%

Table 3 demonstrates that the actual reaction of a single pile is only about 36% of the resisting capacity in this project. It's safe to not consider base shear resisting capacity of piles in design. Therefore, such a method offers substantial opportunity for reducing the steel reinforcement requirement.

6. Conclusions

Dual-purpose diaphragm walls have been widely used in China, especially in Shanghai. It was proved to be a technically and economically viable foundation system in structural support when using the rigid diaphragm to bear partial vertical and horizontal loading.

And we can conclude that:

1. The simple method proposed to solve this problem is reasonable. When the friction between the diaphragm and the soil is neglected, the result is conservative.

2. The results of numerical analysis showed that the actual reaction of a single pile is 36% of its resisting capacity while the diaphragm walls bear most of the base shear. For similar project, we can use the diaphragm to bear partial vertical and horizontal loading. But, in actual project we should verify it before making a judgment.

3. Whether the diaphragm can bear the horizontal loading is still a controversial question, and less engineering can reference. Under these circumstances, a full building modeling providing a more accurate soil–structure interaction, is required. This paper may provide some 'benchmark values' to engineers.

7. Acknowledgements

The authors are grateful for the supports from the Shanghai Excellent Discipline Leader Program (No.14XD1423900) and Key Technologies R & D Program of Shanghai (Grant No. 09dz1207704).

8. References

Chen, Q.Z., Xu, L.Y., Xu, C.J., and Xu, Y.L. (2015), "Optimal design in deep excavation engineering adopting dual-purpose diaphragm walls retaining", *Chinese Journal of Underground Space and Engineering*, 11(1):189-194.

El-Razek, M. (1999), "New Method for Construction of Diaphragm Walls", J. Journal of Construction Engineering and Management, 125(4), 233-241.

Wang W.D., and Weng Q.P. (2005), “Some Key Techniques for the design of dual-purpose diaphragm wall”, *Chinese Journal of Underground Space and Engineering*, 1(4):574-578.

Sun, F., Xu, Y.Q, and Zhang, J.W. (2014), “Design and calculation of vertical bearing capacity of diaphragm wall”. *Chinese Journal of Geotechnical Engineering*, 36(2):154-158.

Ng, C.W.W, Lings M.L., Simpson B., and Nash, D.F.T. (1995), “An approximate analysis of the three dimensional effects of diaphragm wall installation”, *Géotechnique*, 45(3):497–507.

Chu, E.H., Hu, S. (2014), “Design optimization of underground subway station diaphragm walls using numerical modeling”, *Geo-Congress 2014 technical papers*, *ASCE*: 3122-3132.

Comodromos E. M. , Papadopoulou M. C., and Konstantinidis G. K.(2013), “Effects from diaphragm wall installation to surrounding soil and adjacent buildings”, *Computer and Geotechnics*, 53(1):106-121.